RSC Advances

PAPER

View Article Online
View Journal | View Issue

Cite this: *RSC Adv.*, 2016, **6**, 21948

Impact of van der Waal's interaction in the hybrid bilayer of silicene/SiC†

Sandeep Nigam,*[a] Chiranjib Majumder[a] and Ravindra Pandey[b]

Received 5th January 2016
Accepted 14th February 2016

DOI: 10.1039/c6ra00225k

www.rsc.org/advances

Electronic structure calculations based on density functional theory find a presence of noticeable interlayer van der Waal interaction in a hybrid bilayer consisting of a silicene and SiC monolayer sheet with the binding energy of 45 meV per atom. This interlayer interaction also leads to significant changes in the nature of chemical bonding, thereby inducing a curvature in the erstwhile planar SiC sheet. Subsequently, modifications in charge distribution at the interface produce a dissimilar chemical environment for two sub lattices of silicene which opens the band gap in the heterogeneous bilayer system. Application of an external electric field is found to linearly modulate the band gap of the silicene/SiC bilayer indicating its potential use in nanoscale devices.

1. Introduction

Atomic layers of group-IV elements with reduced dimensionality have been of great importance due to their remarkable electronic and magnetic properties for advanced technology applications.[1–8] Although C and Si are group-IV elements, two dimensional (2D) monolayer sheets exhibit different properties as graphene has a planar honeycomb structure, and silicene is stable only if a small buckling ($\approx$0.44 Å) is present.[9–29] The buckled nature of silicene has led to novel properties such as the spin Hall effect,[18,19] adsorption of dopant atoms,[20,21] and modulation of its band gap under an external electric-field.[13,14,22] Graphene and silicene show close similarity in their electronic structures in terms of linear dispersion in the band structure around the Fermi level marking the presence of massless relativistic electrons and an extremely high charge carrier mobility.[10,11] The structural diversity present in carbon-based materials is driven by the degree of hybridization of the valence 2s and 2p orbitals. The hybridization varies from pure sp^2 to sp^3 (including quasi-sp^2 or sp^3 hybridization), which makes these systems adopt a planar, nonplanar or coiled sheet structure.[30,31] Similar to carbon, silicon also has four valence electrons, but Si prefers to be in a sp^3 hybridized state rather than a sp^2 hybridized state.[16,17,31,32] Interestingly, when Si and C are merged to form a SiC monolayer sheet, there exists a preference for a planar honeycomb structure with both Si and C in a sp^2 hybridized state, along with strong π-bonding through perpendicular p_z orbitals.[33–37]

Modulation of the band gap with the help of geometrical strain or an external electric field makes 2D monolayer sheets particularly interesting materials for device applications at the nanoscale.[38–50] For example structurally functionalized silicene has been reported to show ferromagnetic ordering.[42,43] A bilayer system thus provides an additional variable in terms of the degree of interlayer interaction which can be helpful in tailoring the properties for desired applications. For example, a graphene monolayer remains a zero-gap material under an external electric field but a finite band gap appears for bilayer and multilayer graphene.[44,45] Recently Zhang *et al.* showed stacking of silicene on a Sc_2CF_2 monolayer leads to band gap opening of silicene in the range of 36–48 meV.[46] Our research group has recently investigated the electronic properties of hybrid bilayers consisting of silicene/graphene and silicene/BN monolayers suggesting an asymmetrical modulation of the band gap by the external electric field.[50] In this paper, we now consider a monolayer sheet of SiC knowing that SiC is reported to be an excellent insulating substrate for the epitaxial growth of graphene[51–54] together with the fact that electrons in a graphene/SiC system are Dirac fermions.[55,56] In the scientific literature, there are a few reports available on silicene interacting with SiC.[15,57] It has been found that the Dirac cone of silicene is nearly retained on the Si-terminated SiC (0001) surface but silicene becomes metallic when it is placed on a C-terminated surface due to a decline of the Fermi level.[15] Since a 2D monolayer sheet of SiC is quite different from a surface of SiC in terms of the nature of its chemical bonds, it is worth investigating the interaction of silicene with a SiC monolayer sheet in a hybrid silicene/SiC bilayer system. Section 2 describes the computational method. The results are discussed in Section 3 and a summary of the work is provided in Section 4.

[a]*Chemistry Division, Bhabha Atomic Research Centre, Trombay, 400085, Mumbai, India. E-mail: snigam.jpr@gmail.com; drchiranjib@gmail.com*

[b]*Department of Physics, Michigan Technological University, 49931, Houghton, Michigan, USA. E-mail: pandey@mtu.edu*

† Electronic supplementary information (ESI) available. See DOI: 10.1039/c6ra00225k

2. Computational method

Electronic structure calculations were performed using the plane-wave based pseudopotential approach in the framework of density functional theory as implemented in the Vienna *ab initio* Simulation Package (VASP).[58,59] The electron–ion interaction was described by the projector augmented wave (PAW) method[60] and the Perdew–Burke–Ernzerhof (PBE) generalized gradient approximation was used.[61] The van der Waals corrections (DFT-D2) within the PBE functional proposed by Grimme were also employed.[62] The vacuum distance of 15 Å was used to reduce the interactions between the periodic images in the supercell model. The cut-off energy for the plane wave basis set was fixed at 520 eV. The positions of atoms were optimized without any constraint until the convergence of the force on each atom was less than 0.01 eV $Å^{-1}$. The total energy convergence was tested with respect to the plane-wave basis set size and the cell size, leading its accuracy to be within 1 meV. The Monkhorst–Pack scheme is used to sample the Brillouin zone with a (15 × 15 × 1) *k*-mesh. A co-periodic lattice is used to simulate the bilayer system which minimizes the lattice mismatch between silicene with the SiC monolayer. The co-periodic lattice consisted of (4 × 4) silicene (32 Si atoms) with (5 × 5) SiC (25 C atoms and 25 Si atoms) yielding the lattice mismatch to be about ~0.53%. Note that the modeling parameters employed have reproduced the results of previous studies on pristine silicene[14,15] and a SiC monolayer[63] demonstrating their accuracy and reliability. For example, the calculated lattice constants of a pristine SiC monolayer and silicene are 3.09 and 3.85 Å, respectively (Fig. S1 of ESI†). Buckling of pristine silicene (measured from the vertical distance between the two sub-lattices) is calculated to be 0.47 Å in agreement with previous[14,15] results based on density functional theory. In the case of the pristine SiC sheet, a significant electronic charge (~4e) is transferred from Si to C in the lattice (Fig. S2 of ESI†) in excellent agreement with previous results.[63]

3. Results and discussion

In the equilibrium configuration of a silicene/SiC bilayer, the calculated results find the pristine planar SiC sheet to be rippled with a few Si and C atoms moving out of the plane by 0.25–0.5 Å from original molecular plane of the pristine sheet (Fig. 1, Table 1). The intra-planar Si–Si bond (*i.e.* R_{Si-Si} ≈ 2.27 Å) nearly remains the same, but the buckled height of the supported silicene (≈0.5–0.6 Å) slightly changes with regard to the pristine silicene (≈0.47 Å). The interlayer distance ($R_{interlayer}$) for the bilayer is 3.47 Å. The interlayer distance has been obtained from the average vertical distance between the silicene and the SiC sheet. The calculated binding energy/atom with respect to the constituent monolayers [*i.e.* $E_{binding} = (E_A + E_B - E_{AB})$/total no. of atoms present in both the sheets] is 45 meV per atom‡ which is much higher than the silicene/graphene and silicene/BN bilayers, respectively.[50] In order to make sure that the observed rippling is not simply an artifact of the van der Waals corrections (DFT-D2) term, additional calculations were carried out in absence of D2 correction. The calculated DFT results also show rippling with significantly smaller (average) binding energy. Note that the binding energy for the AB-stacked graphene bilayer is 25 meV per atom whereas that of the AB-stacked graphene/BN bilayer is 26 meV per atom.[50] Thus, it appears that van der Waal interactions between the SiC sheet and silicene are much stronger than other 2D bilayers and perhaps this has led to the calculated curvature in the SiC sheet. It is worth mentioning that the equilibrium configuration of a co-periodic silicene/SiC lattice was obtained by carrying out the geometry optimization without any constraint, hence the possibility of curvature in the SiC sheet due to geometrical strains can easily be ruled out. The charge iso-density surface shows a finite overlap of charge density contours at the interface (Fig. S3 of ESI†), further confirming the presence of a strong interaction at the interface of the two sheets and hence understandably, the induced curvature in the SiC sheet is driven by these van der Waal forces exerted only by the silicene sheet in the hybrid bilayer. Further it is important to note that during the binding of two sheets in terms of per unit surface area, the binding energy is 16 meV $Å^{-2}$.

Next, we investigate the electronic structure of the silicene/SiC bilayer knowing that the electronic properties of the 2D bilayers can be modulated depending upon the nature of bonding at the interface. Fig. 2 shows the projected density of states (PDOS) of the SiC monolayer, silicene and silicene/SiC bilayer systems. In the pristine SiC sheet (Fig. 2a and c) s, p_x, and p_y orbitals are merged with each other due to sp^2 hybridization, and p_z orbitals do not participate in the orbital hybridization. The valance band states near the Fermi level are dominated by C p_z orbitals, while the conduction band states near the Fermi level have a major contribution from Si p_z orbitals. Previously, it has been reported that even though Si and C in bulk SiC favor sp^3 hybridization, SiC sheets prefer sp^2-hybridized features resembling graphene and strong π-bonding through perpendicular p_z orbitals has been attributed to its 2D planar honeycomb structure.[35,63] The results obtained in the present work are in line with previous reports.[35,63] Contrary to pristine SiC, when an SiC sheet interacts with silicene (Fig. 2b

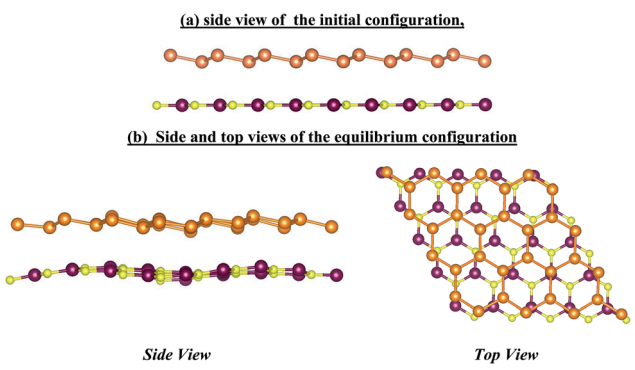

Fig. 1 A ball and stick diagram of the silicene/SiC bilayer (Si of SiC sheet: purple, C: yellow, Si of silicene sheet: orange).

‡ The binding energy calculated with a vacuum layer of 20 Å in the supercell is 44.8 meV per atom.

Table 1 The structural and electronic properties of the equilibrium configurations of silicene, the SiC monolayer sheet and silicene/SiC bilayer

System	Intra-planar distance $R_{intraplaner}$ (Å)	Interlayer separation (average) $R_{interlayer}$ (Å)	Binding energy (meV per atom)	Band gap (meV)
Silicene/SiC-bilayer	$R_{Si-Si} = 2.28–2.29$, $R_{Si-C} = 1.77–1.78$	3.45	45	180
Silicene-monolayer	$R_{Si-Si} = 2.27$	—	—	~0
SiC-monolayer	$R_{Si-C} = 1.79$	—	—	2560

and d), the electronic structure is significantly influenced as all valance orbitals (*i.e.* s, p_x, p_y and p_z) participate in a supposed sp^3 kind of hybridization in the bilayer. In particular, the p_z orbitals of the SiC sheet are greatly affected by the silicene sheet inducing ripples/curvature in the planar honeycomb sheet.

In comparison to a pristine SiC sheet, pristine silicene (Fig. 2e) shows sp^3 bonding, and hence has a buckled structure. Importantly, the electronic structure of silicene shows semi-metallic behavior having a Dirac cone similar to that of graphene. In line with a previous report, we also find silicene to have a zero band gap. But this is not the case with the silicene/SiC bilayer where an opening of the band gap (≈0.18 eV) is predicted (Table 1, Fig. S4 of ESI†). Note that the band gaps of the silicene/BN and silicene/graphene bilayers with an interlayer separation around 3.3 Å are reported to be to 47 and 51 meV, respectively.[50]

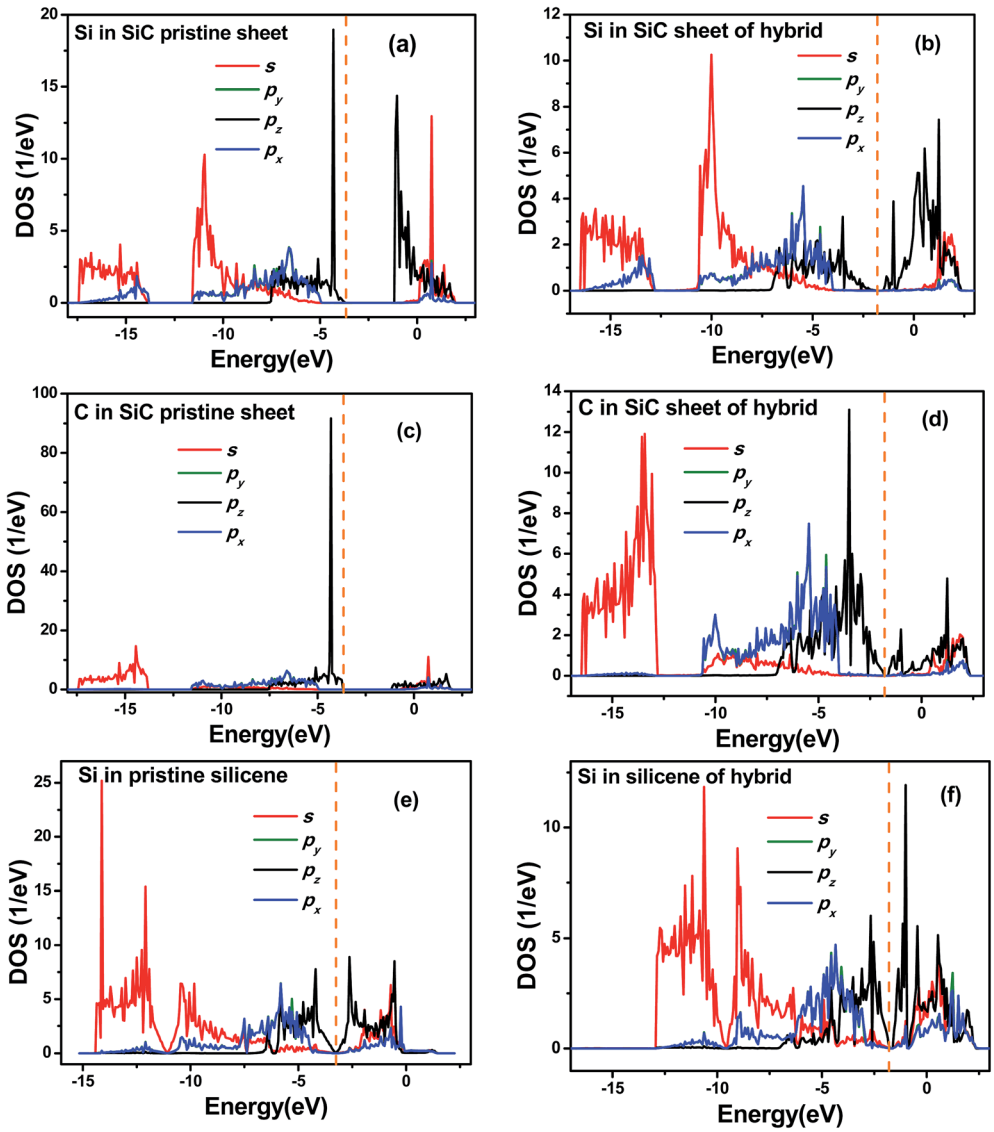

Fig. 2 The orbital decomposed projected density of states for the silicene/SiC bilayer. The vertical dotted line corresponds to Fermi level.

Fig. 3 displays the charge density difference ($\Delta\rho$) which is defined as ρ (silicene/SiC) − ρ (SiC) − ρ (silicene) with ρ (SiC/silicene) being the charge density of the bilayer. It clearly shows that charge density is redistributed by forming electron-rich and electron deficient regions at the interface. It is important to note here that two sub lattices of silicene have different chemical environments as an upper Si atom has an electron-rich blue region around it while a lower Si atom has an electron-deficient grey region in the vicinity (*viz.* Fig. 3). Therefore, the dissimilar chemical environments of the two sub-lattices of silicene lead to an opening of the band gap in the hybrid bilayer. This is also the case with graphene where the broken sublattice symmetry leads to an opening of its band gap.[47,48,64–66]

Modifications in the band structure of silicene in the bilayer are shown in Fig. 4(a) where the valence band appears to shift to a higher energy without changing its shape. In contrast, the shape of the conduction band as well as its location is significantly affected in the bilayer. The influence of the SiC sheet on the Si p_z states of silicene near the Fermi level is shown in Fig. 4(b) suggesting it to be more pronounced in the conduction region. Thus, the calculated results firmly establish the opening of the band gap in silicene due to the appearance of the van der Waals interactions in the silicene/SiC hybrid bilayer.

Since application of an external electric field (E_{field}) can further modulate the charge density, and hence can tune the band gap, we now perform band structure calculations under the application of the perpendicular electric field for the bilayer. The calculated results show that the silicene/SiC bilayer exhibits approximately linear modulation of the band gap with E_{Field} in the range from −0.4 to 0.4 V Å^{-1} as shown in Fig. 5. Note that the positive value of E_{Field} refers to application of the electric field from bottom to top of the bilayer system. In the presence of +0.4 V Å^{-1}, the difference between the chemical environments (*i.e.* charge distribution around the upper and lower Si atoms of silicene) further increases yielding the band gap of 0.22 eV (Fig. S5 of ESI†). Modulation of the band gap of the bilayer is indeed governed by movement of the conduction band states of silicene (Fig. 6(a)) due mainly to modifications in the p_z states as shown in the PDOS given in (Fig. 6(b)).

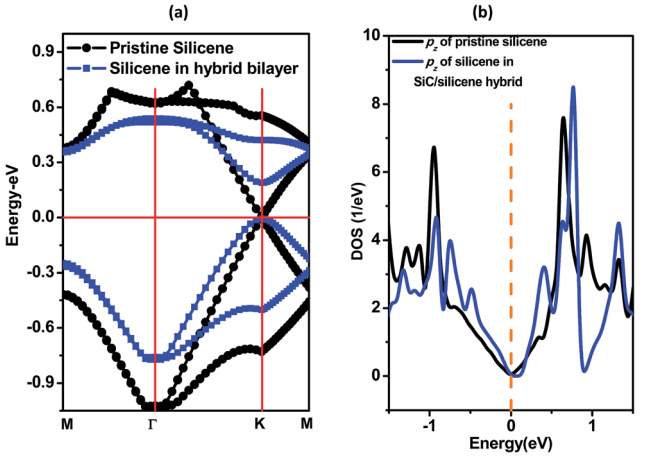

Fig. 4 (a) Band structure of a silicene/SiC bilayer near the Fermi level (only two conduction and two valence bands are presented for clarity) (b) projected density of states for the silicene/SiC bilayer. The Fermi level is aligned to zero.

4. Summary

In summary, the calculated results based on density functional theory show that a pristine planar SiC sheet gets rippled after interaction with silicene in the silicene/SiC hybrid bilayer. This is primarily due to deviation of the hybridization state of the Si atom of the SiC sheet from sp^2 due to fusion with the p_z states. Interactions between silicene and the SiC monolayer sheet lead to redistribution of the charge density at the interface especially associated with the Si-p_z states, which subsequently induce a finite band gap in the silicene. This is further confirmed by the linear modulation of the band gap under an electric field applied perpendicular to the silicene/SiC bilayer. We believe

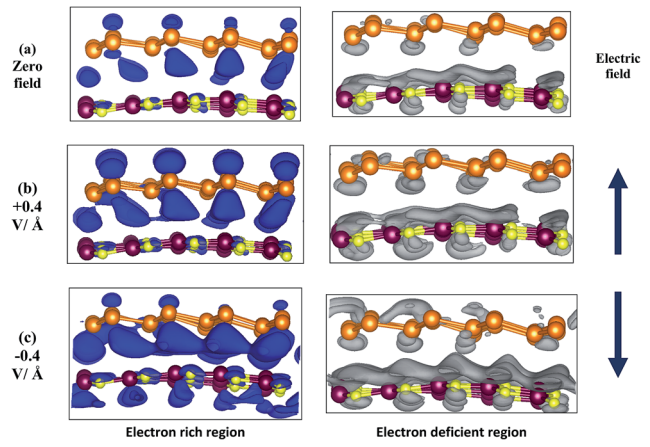

Fig. 3 The charge density difference ($\Delta\rho$) of silicene/SiC bilayer for E_{Field} = 0, +0.4 V Å^{-1}, and −0.4 V Å^{-1} using the contours of 6 × 10^{-3} electron per bohr^3. Blue: increase in the charge density, gray: decrease in the charge density.

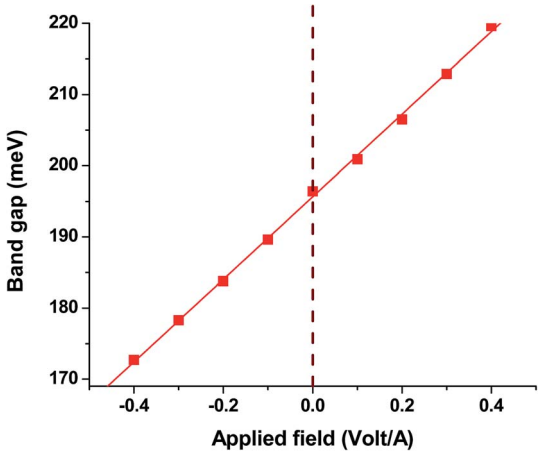

Fig. 5 Silicene/SiC bilayer: variation of the band gap with the perpendicular electric field. The positive value of E_{Field} refers to the direction of the electric field from bottom to top of the bilayer system.

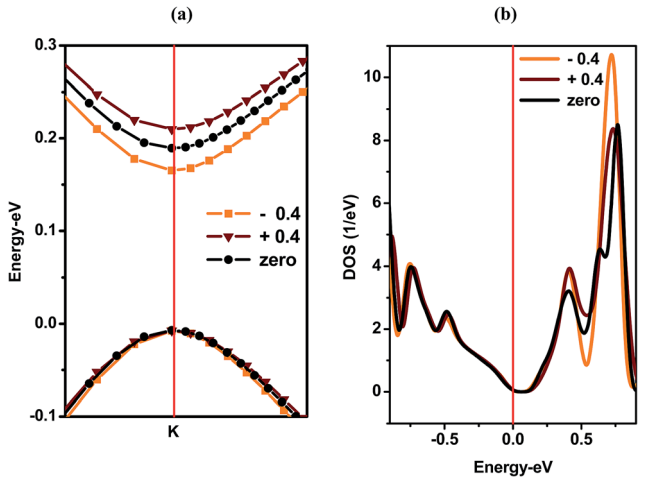

Fig. 6 Silicene/SiC bilayer: influence of electric field on (a) the band structure of near Fermi level (only one conduction and valence band are presented for clarity). (b) p_z orbital of silicene. The Fermi level is aligned to zero.

that the results of our study will help in advancing the fundamental understanding of silicene-based two dimensional materials towards their incorporation in the next-generation microelectronic industry.

Acknowledgements

SN acknowledges the support of the Michigan Technological University. Authors (SN and CM) are grateful to the computer division, BARC for providing the Anupum supercomputing facility. Superior, a high performance computing cluster at Michigan Technological University, was used in obtaining some of the results presented in this paper.

References

1 P. Miro, M. Audiffred and T. Heine, *Chem. Soc. Rev.*, 2014, **43**, 6537.
2 F. Bonaccorso, L. Colombo, G. Yu, M. Stoller, V. Tozzini, A. C. Ferrari, R. S. Ruoff and V. Pellegrini, *Science*, 2015, **347**, 6217, DOI: 10.1126/science.1246501.
3 S. Z. Butler, S. M. Hollen, L. Cao, Y. Cui, J. A. Gupta, H. R. Gutierrez, T. F. Heinz, S. S. Hong, J. Huang, A. F. Ismach, E. Johnston-Halperin, M. Kuno, V. V. Plashnitsa, R. D. Robinson, R. S. Ruoff, S. Salahuddin, J. Shan, L. Shi, O. M. G. Spencer, M. Terrones, W. Windl and J. E. Goldberger, *ACS Nano*, 2013, **7**, 2898.
4 F. Yavari, C. Kritzinger, C. Gaire, L. Song, H. Gullapalli, T. Borca-Tasciuc, P. M. Ajayan and N. Koratkar, *Small*, 2010, **6**, 2535.
5 A. H. Castro Neto, F. Guinea, N. M. R. Peres, K. S. Novoselov and A. K. Geim, *Rev. Mod. Phys.*, 2009, **81**, 109.
6 K. Geim, *Science*, 2009, **324**, 1530.
7 Q. Tang and Z. Zhou, *Prog. Mater. Sci.*, 2013, **58**, 1244.
8 Y. Jing, Z. Zhou, C. R. Cabrera and Z. Chen, *J. Mater. Chem. A*, 2014, **2**, 12104.
9 R. W. Zhang, C. W. Zhang, W. X. Ji, S. J. Hu, S. S. Yan, S. S. Li, P. Li, P. J. Wang and Y. S. Liu, *J. Phys. Chem. C*, 2014, **118**, 25278.
10 J. H. Kim and Z. Lee, *Applied Microscopy*, 2014, **44**, 123.
11 S. Balendhran, S. Walia, H. Nili, S. Sriram and M. Bhaskaran, *Small*, 2015, **11**, 640.
12 S. Cahangirov, M. Topsakal, E. Aktürk, H. Şahin and S. Ciraci, *Phys. Rev. Lett.*, 2009, **102**, 236804; S. Cahangirov, V. O. Özçelik, L. Xian, J. Avila, S. Cho, M. C. Asensio, S. Ciraci and A. Rubio, *Phys. Rev. B: Condens. Matter Mater. Phys.*, 2014, **90**(3), 035448.
13 Z. Ni, Q. Liu, K. Tang, J. Zheng, J. Zhou, R. Qin, Z. Gao, D. Yu and J. Lu, *Nano Lett.*, 2012, **12**, 113.
14 N. D. Drummond, V. Zólyomi and V. I. Fal'ko, *Phys. Rev. B: Condens. Matter Mater. Phys.*, 2012, **85**, 075423.
15 H. Liu, J. Gao and J. Zhao, *J. Phys. Chem. C*, 2013, **117**, 10353.
16 D. Jose and A. Datta, *Acc. Chem. Res.*, 2014, **47**(2), 593.
17 D. Jose and A. Datta, *J. Phys. Chem. C*, 2012, **116**, 24639.
18 M. Ezawa, *Phys. Rev. Lett.*, 2012, **109**, 055502.
19 A. Dyrdal and J. Barnas, *Phys. Status Solidi RRL*, 2012, **6**, 340.
20 X. Lin and J. Ni, *Phys. Rev. B: Condens. Matter Mater. Phys.*, 2012, **86**, 075440.
21 H. Sahin and F. M. Peeters, *Phys. Rev. B: Condens. Matter Mater. Phys.*, 2013, **87**, 085423.
22 Y. Liang, V. Wang, H. Mizuseki and Y. Kawazoe, *J. Phys.: Condens. Matter*, 2012, **24**, 455302.
23 R. Li, Y. Han and J. Dong, *Phys. Chem. Chem. Phys.*, 2015, **17**, 22969.
24 P. A. Denisa, *Phys. Chem. Chem. Phys.*, 2015, **17**, 5393.
25 R. Wang, X. Pi, Z. Ni, Y. Liua and D. Yanga, *RSC Adv.*, 2015, **5**, 33831.
26 X. Wang, H. Liu and S. T. Tu, *RSC Adv.*, 2015, **5**, 65255.
27 X. S. Ye, Z. G. Shao, H. Zhao, L. Yang and C. L. Wang, *RSC Adv.*, 2014, **4**, 37998.
28 Q. Peng, X. Wen and S. De, *RSC Adv.*, 2013, **3**, 13772.
29 J. Liu and W. Zhang, *RSC Adv.*, 2013, **3**, 21943.
30 K. R. S. Chandrakumar, K. Srinivasu and S. K. Ghosh, *J. Phys. Chem. C*, 2008, **112**, 15670.
31 L. Sun, Y. Li, Z. Li, Q. Li, Z. Zhou, Z. Chen, J. Yang and J. G. Hou, *J. Chem. Phys.*, 2008, **129**, 174114.
32 S. Banerjee, S. Nigam, C. G. S. Pillai and C. Majumder, *Int. J. Hydrogen Energy*, 2012, **37**, 3733.
33 E. Bekaroglu, M. Topsakal, S. Cahangirov and S. Ciraci, *Phys. Rev. B: Condens. Matter Mater. Phys.*, 2010, **81**, 075433.
34 M. Yu, C. S. Jayanthi and S. Y. Wu, *Phys. Rev. B: Condens. Matter Mater. Phys.*, 2010, **82**, 075407.
35 T. Y. Lu, X. X. Liao, H. Q. Wang and J. C. Zheng, *J. Mater. Chem.*, 2012, **22**, 10062.
36 X. Yan, Z. Xin, L. Tian and M. Yu, *Comput. Mater. Sci.*, 2015, **107**, 8.
37 J. W. Feng, Y. J. Liu and J. X. Zhao, *J. Mol. Graphics Modell.*, 2015, **60**, 132.
38 S. K. Banerjee, L. F. Register, E. Tutuc, D. Basu, S. Kim, D. Reddy and A. H. MacDonald, *Proc. IEEE*, 2010, **98**, 2032.

39 V. M. Pereira and A. H. C. Neto, *Phys. Rev. Lett.*, 2009, **103**, 046801.
40 F. Schwierz, *Nat. Nanotechnol.*, 2010, **5**, 487.
41 B.-R. Wu, *Appl. Phys. Lett.*, 2011, **98**, 263107.
42 C.-W. Zhang and S.-S. Yan, *J. Phys. Chem. C*, 2012, **116**, 4163.
43 F.-B. Zheng and C.-W. Zhang, *Nanoscale Res. Lett.*, 2012, **7**, 422.
44 D. Kaplan, V. Swaminathan, G. Recine, R. Balu and S. Karna, *J. Appl. Phys.*, 2013, **113**, 183701.
45 E. V. Castro, K. S. Novoselov, S. V. Morozov, N. M. R. Peres, J. M. B. Lopes dos Santos, J. Nilsson, F. Guinea, A. K. Geim and A. H. Castro Neto, *J. Phys.: Condens. Matter*, 2010, **22**, 175503.
46 H. Zhao, C.-W. Zhang, S. Li, W. Ji and P. Wang, *J. Chem. Phys.*, 2015, **117**, 085306.
47 S. Tang, J. Yu and L. Liu, *Phys. Chem. Chem. Phys.*, 2013, **15**, 5067.
48 R. Balu, X. Zhong, R. Pandey and S. P. Karna, *Appl. Phys. Lett.*, 2012, **100**, 052104.
49 X. Zhong, Y. K. Yap, R. Pandey and S. P. Karna, *Phys. Rev. B: Condens. Matter Mater. Phys.*, 2011, **83**, 193403.
50 S. Nigam, S. K. Gupta, C. Majumder and R. Pandey, *Phys. Chem. Chem. Phys.*, 2015, **17**, 11324.
51 A. Mattausch and O. Pankratov, *Phys. Rev. Lett.*, 2007, **99**, 076802.
52 J. Sforzini, L. Nemec, T. Denig, B. Stadtmüller, T.-L. Lee, C. Kumpf, S. Soubatch, U. Starke, P. Rinke, V. Blum, F. C. Bocquet and F. S. Tautz, *Phys. Rev. Lett.*, 2015, **114**, 106804.
53 K. Yamasue, H. Fukidome, K. Funakubo, M. Suemitsu and Y. Cho, *Phys. Rev. Lett.*, 2015, **114**, 226103.
54 V. W. Brar, Y. Zhang, Y. Yayon, T. Ohta, J. L. McChesney, A. Bostwick, E. Rotenberg, K. Horn and M. F. Crommie, *Appl. Phys. Lett.*, 2007, **91**, 122102.
55 C. Berger, Z. Song, X. Li, X. Wu, N. Brown, C. Naud, D. Mayou, T. Li, J. Hass, A. N. Marchenkov, E. H. Conrad, P. N. First and W. A. de Heer, *Science*, 2006, **312**, 1191.
56 T. Ohta, A. Bostwick, T. Seyller, K. Horn and E. Rotenberg, *Science*, 2006, **313**, 951.
57 H. J. Wu, M. T. Hoang, Y. Li and P. N. First, http://meetings.aps.org/link/BAPS.2015.MAR.Y8.8.
58 G. Kresse and J. Furthmuller, *Phys. Rev. B: Condens. Matter Mater. Phys.*, 1996, **54**, 11169; *Comp. Mater. Sci.*, 1996, **6**, 15; D. Vanderbilt, *Phys. Rev. B: Condens. Matter Mater. Phys.*, 1990, **41**, 7892.
59 G. Kresse and D. Joubert, *Phys. Rev. B: Condens. Matter Mater. Phys.*, 1999, **59**, 1758.
60 P. E. Blochl, *Phys. Rev. B: Condens. Matter Mater. Phys.*, 1994, **50**, 17953.
61 J. P. Perdew, K. Burke and M. Ernzerhof, *Phys. Rev. Lett.*, 1996, **77**, 3865.
62 S. Grimme, *J. Comput. Chem.*, 2006, **27**(15), 1787.
63 H. Sahin, S. Cahangirov, M. Topsakal, E. Bekaroglu, E. Akturk, R. T. Senger and S. Ciraci, *Phys. Rev. B: Condens. Matter Mater. Phys.*, 2009, **80**, 155453.
64 Y. Cai, C.-P. Chuu, C. M. Wei and M. Y. Chou, *Phys. Rev. B: Condens. Matter Mater. Phys.*, 2013, **88**, 245408.
65 A. Lherbier, A. R. Botello-Méndez and J.-C. Charlier, *Nano Lett.*, 2013, **13**, 1446.
66 I. Deretzis and A. La Magna, *Phys. Rev. B: Condens. Matter Mater. Phys.*, 2014, **89**, 115408.